

Link: <http://charles.karney.info/biblio/karney77c.html>

STOCHASTIC ION HEATING BY A PERPENDICULARLY
PROPAGATING ELECTROSTATIC WAVE

C. F. F. Karney, A. Bers

Plasma Research Report

PRR 76/24
July 1976

2. STOCHASTIC ION HEATING BY A PERPENDICULARLY PROPAGATING ELECTROSTATIC WAVE

U. S. Energy Research and Development Administration (Contract E(11-1)-3070)

Charles F. F. Karney, Abraham Bers

Introduction

In RLE Progress Report No. 117 (pp. 193-197) we considered the nonlinear motion of an ion in a perpendicularly propagating electrostatic wave. We found the condition under which the ion becomes momentarily trapped by the wave and so exchanges significant energy with the wave. In this report we examine the subsequent behavior of the ions and the conditions under which the ions are stochastically heated.

Hamiltonian Formulation

To study the long-term behavior of an ion, it is convenient to work with its Hamiltonian. The applied electric field is $\hat{y}E \cos(ky - \omega t - \phi)$. The equations of motion (discussed in our previous report) are

$$\ddot{y} + y = a \cos(y - vt - \phi); \quad \dot{x} = y \tag{1}$$

where lengths are normalized to $1/k$ and times to $1/\Omega$, $a = qkE/\Omega^2 m$, and $v = \omega/\Omega$.

By evaluating the Hamiltonian equations, it can be verified that the Hamiltonian is $1/2(p_y^2 + y^2) - a \sin(y - vt - \phi)$. In order to work with a conservative system, we recast the Hamiltonian into

$$H = J_1 + \nu J_2 - a \sin(\sqrt{2J_1} \sin w_1 - w_2), \quad (2)$$

where J_1, w_1 , and J_2, w_2 are conjugate action angle variables, and $p_y = \sqrt{2J_1} \cos w_1$, $y = \sqrt{2J_1} \sin w_1$. The Hamiltonian equation $\dot{w}_2 = \partial H / \partial J_2$ may be integrated directly to give $w_2 = \nu t + \phi$. Thus w_2 is the wave phase and J_2 its conjugate action. Equation 2 may be viewed as describing two harmonic oscillators (the ion with frequency 1 described by J_1, w_1 and the wave with frequency ν described by J_2, w_2) coupled by the last term of the equation.

Phase Plane Trajectories

We begin our study of an ion with the Hamiltonian given by Eq. 2 by solving numerically for its trajectory in phase space. To picture the trajectory most easily, we plot only the cross section defined by $w_1 = \pi$ (the ion traveling in the $-y$ direction). We plot $r (= \sqrt{2J_1})$ against w_2 for each crossing of the $w_1 = \pi$ plane where r is the normalized velocity of the ion. Figure X-29 shows such plots for $\nu = 30.11$ and 30.23 , and $a = 1, 2$, and 3 . The trajectories of 15 particles are followed in each case. In these plots the condition that the ions travel at the wave phase velocity is given by $r = \nu$. If $r < \nu - \sqrt{a}$, we expect negligible interaction with the wave. With $a = 1$ the trajectories all lie on smooth curves. The existence of such continuous curves indicates that with small but finite a there is a new conserved quantity. (With $a = 0$ the trajectories would all lie on horizontal straight lines, since J_1 is then a conserved quantity.) At $a = 2$ we see the formation of "islands." The islands are first order for $\nu = 30.11$ but fourth order for $\nu = 30.23$ (in the latter case the particle takes four crossings of the $w_1 = \pi$ plane to return to the island on which it started). Outside the islands we see the beginning of stochastic behavior, but the stochastic regions are separated from one another by coherent regions, which prevents the movement of particles from one stochastic region to another. Finally, at $a = 3$, the stochastic regions have begun to merge, although island formations are still evident.

Conditions for Island Formation

Following Walker and Ford,¹ we transform our Hamiltonian into one that is cyclic in the angle variables and so obtain conserved actions. (The technique is valid only for small a .) We begin by expanding the last term of Eq. 2 in a Fourier series.

$$H = J_1 + \nu J_2 - a \sum_{m=-\infty}^{\infty} J_m(\sqrt{2J_1}) \sin(mw_1 - w_2). \quad (3)$$

Here J_m is a Bessel function of the first kind. Using the generating function²

$$F_2 = \mathcal{J}_1^{w_1} + \mathcal{J}_2^{w_2} - a \sum_m \frac{J_m(\sqrt{2J_1}) \cos(mw_1 - w_2)}{m - \nu}, \quad (4)$$

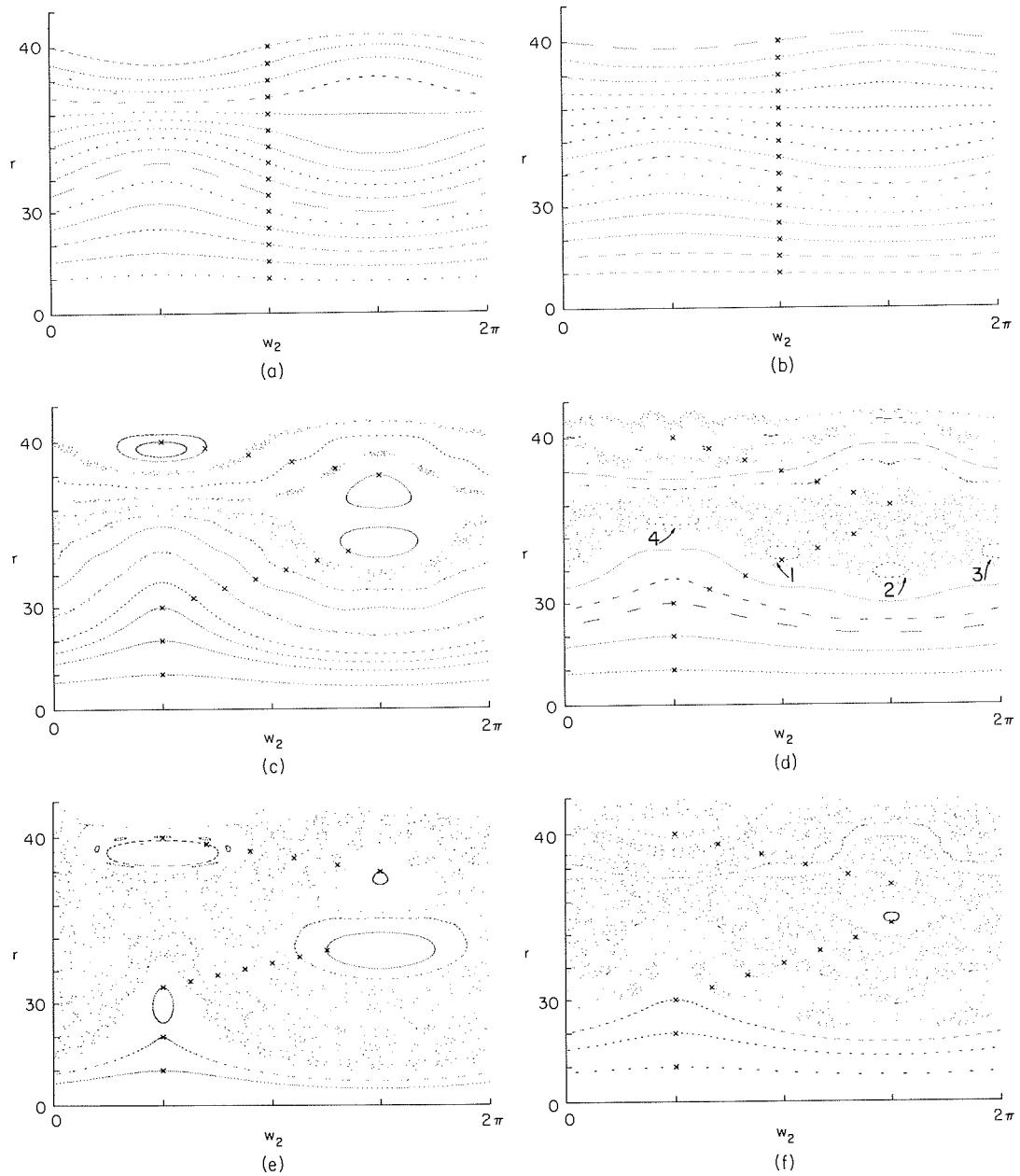


Fig. X-29. $w_1 = \pi$ cross section of phase space. Crosses (X) indicate initial conditions, dots (●) subsequent crossings. In (d) numbers indicate positions of fourth-order island formations and the order in which they are visited.

- | | |
|--------------------------|--------------------------|
| (a) $\nu = 30.11, a = 1$ | (b) $\nu = 30.23, a = 1$ |
| (c) $\nu = 30.11, a = 2$ | (d) $\nu = 30.23, a = 2$ |
| (e) $\nu = 30.11, a = 3$ | (f) $\nu = 30.23, a = 3$ |

we obtain the following canonical transformation into action-angle variables \mathcal{J}_1 , w_1 and \mathcal{J}_2 , w_2 :

$$J_1 = \frac{\partial F_2}{\partial w_1} = \mathcal{J}_1 + a \sum_m \frac{m J_m(\sqrt{2}\mathcal{J}_1) \sin(mw_1 - w_2)}{m - \nu} \quad (5)$$

$$J_2 = \frac{\partial F_2}{\partial w_2} = \mathcal{J}_2 - a \sum_m \frac{J_m(\sqrt{2}\mathcal{J}_1) \sin(mw_1 - w_2)}{m - \nu}. \quad (6)$$

The transformed Hamiltonian

$$\mathcal{H} = H = \mathcal{J}_1 + \nu \mathcal{J}_2 + a \sum_m [J_m(\sqrt{2}\mathcal{J}_1) - J_m(\sqrt{2}J_1)] \sin(mw_1 - w_2). \quad (7)$$

Under the assumption that the transformation is nearly an identity transformation, i. e., $\mathcal{J}_1 = J_1 + O(a)$,

$$\mathcal{H} = \mathcal{J}_1 + \nu \mathcal{J}_2 + O(a^2), \quad (8)$$

so that \mathcal{J}_1 and \mathcal{J}_2 are approximate constants of the motion. From (5)

$$\mathcal{J}_1 \approx J_1 - a \sum_m \frac{m J_m(\sqrt{2}J_1) \sin(mw_1 - w_2)}{m - \nu}. \quad (9)$$

In order to compare this with the numerical solutions of Fig. X-29, we take $w_1 = \pi$. Equation 9 then reduces to

$$\mathcal{J}_1 \approx J_1 + a \sum_{m=-\infty}^{\infty} \frac{m(-1)^m J_m(\sqrt{2}J_1)}{m - \nu} \sin w_2. \quad (10)$$

In Fig. X-30 we use Eq. 10 to plot curves of constant \mathcal{J}_1 for the parameters in Fig. X-29. We see that the general features of the primary island formation for $\nu = 30.11$ are well predicted by Eq. 10. The higher order islands formed with $\nu = 30.23$ and $a = 2$ are not predicted by Eq. 10, although for $a = 3$ we see the same first-order island that was observed in Fig. X-29.

From Eq. 10 we can derive the condition for primary island formation by setting $\partial \mathcal{J}_1 / \partial w_2 = \partial \mathcal{J}_1 / \partial J_1 = 0$. We find that islands occur where

$$a > \left| \frac{r}{\sum_m \frac{m(-1)^m J'_m(r)}{m - \nu}} \right|. \quad (11)$$

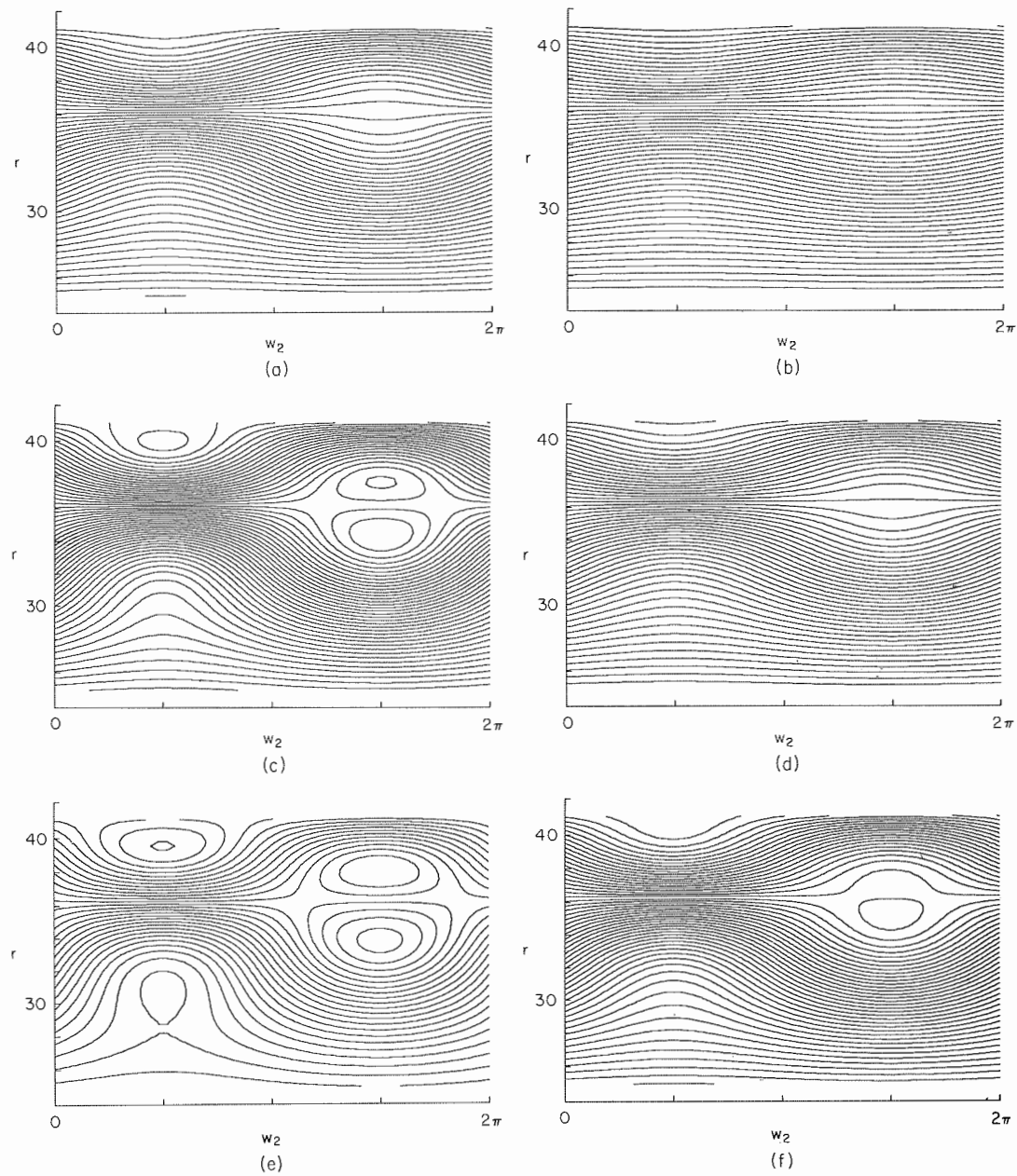


Fig. X-30. Contour plots of the approximate constant of the motion \mathcal{J}_1 (see Eq. 9). Parameters for a-f are the same as in Fig. X-29.

If $\nu \approx n$ (an integer), then Eq. 11 can be simplified to give³

$$a > \left| \frac{r\delta}{nJ'_n(r)} \right|, \quad (12)$$

where $\delta = \nu - n$.

Conditions for Stochasticity

Although we see from Eq. 12 that the field for primary island formation has a strong dependence on δ , the numerical results in Fig. X-29 indicate that the condition for the merging of stochastic regions is insensitive to δ . This stochasticity criterion is most important from the point of view of heating, since it gives the conditions under which an ion can be heated appreciably.

In Fig. X-31 we plot the extent of the connected stochastic regions as a function of a for $\nu = 30.11$ and 30.23 . Since the boundaries of the stochastic region are not necessarily lines of constant r , we plot the intersection of the boundaries with the line $w_2 = 0$.

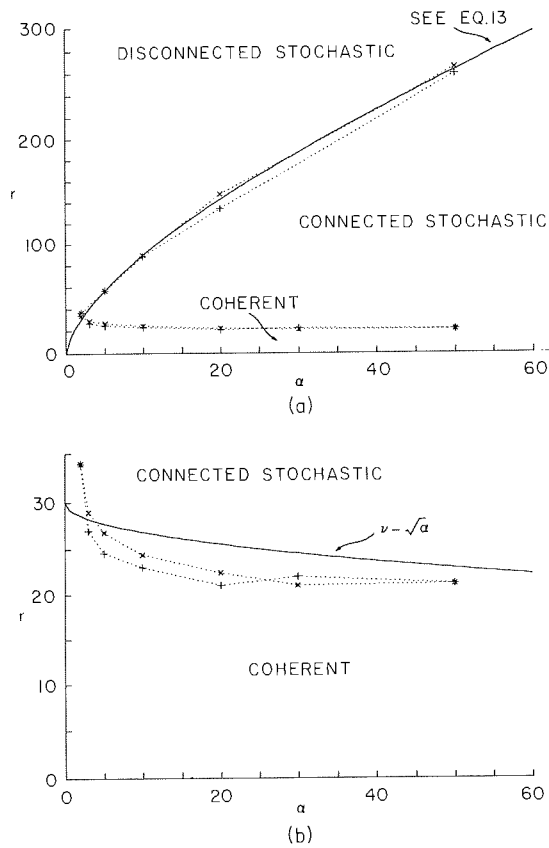


Fig. X-31. (a) Extent of connected stochastic regions as a function of a .
 (b) Lower portion of (a) on an expanded scale.
 Plus (+) indicates $\nu = 30.11$, cross (X) $\nu = 30.23$.

(X. PLASMA DYNAMICS)

We observe only coherent motion for r below the lower curves, and disconnected stochastic regions above the upper curves. We may derive an approximate equation for the upper data points by assuming that Eq. 12 gives the correct scaling of the stochasticity condition with r , although not its scaling with δ . We expand asymptotically the Bessel function in Eq. 12, solve for r , and replace δ with Δ to serve as an adjustable parameter, to obtain

$$r = \left(\frac{an}{\Delta}\right)^{2/3} \left(\frac{2}{\pi}\right)^{1/3}. \tag{13}$$

Equation 13 with $n = 30$ and $\Delta = 0.28$ is shown as a solid curve in Fig. X-31. The close fit suggests that Eq. 13 gives correctly the upper limit to the heating.

Since linear theory shows such a pronounced dependence on δ it is somewhat surprising that Eq. 13 should not depend at all on δ . To understand this, we go back to the linear theory. Consider a particle that at $t = 0$ has $\dot{y} = -r$ and $y = 0$. If the particle equation of motion (1) is integrated along its unperturbed orbit for a time 2π , we find that the change in the particle Larmor radius is

$$\Delta r = \frac{2\pi\nu}{r} a \cos(\nu\pi + \phi) J_\nu(r). \tag{14}$$

(We have approximated the Anger's function arising from this integration by the corresponding Bessel function, since ν is assumed large.) Observe that Eq. 14 does not exhibit a strong δ -dependence (that dependence comes into linear theory when we sum Eq. 14 over many cyclotron periods) and the $\cos(\nu\pi + \phi)$ term constructively or destructively interferes, depending on whether or not ν is integral. Substituting Eq. 13 in Eq. 14, we find that at the upper limit of the stochasticity region we have $\Delta r = 2\pi\Delta \cos(\nu\pi + \phi) \cos(r - \nu\pi/2 - \pi/4)$. Thus in order for the motion to be stochastic, we require that the jump in the Larmor radius which the particle makes in one cyclotron orbit be some fraction of the period of the Bessel function appearing in Eq. 14.

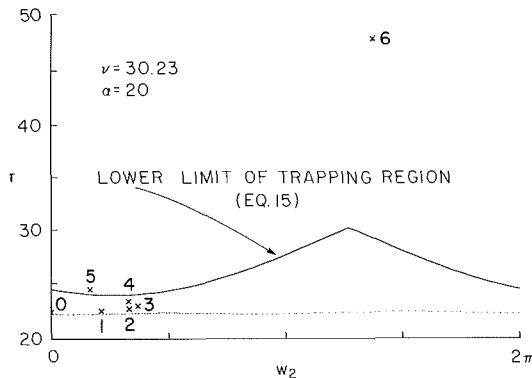


Fig. X-32.

$w_1 = \pi$ cross section of phase space showing the effect of trapping. Dots (\bullet) indicate the particle orbit in the coherent region, crosses (\times) the particle orbit just inside the stochastic region. Numbers refer to successive crossings of the $w_1 = \pi$ plane.

This explanation does not satisfactorily explain the lower set of data in Fig. X-31. Presumably, the reason is that whereas the upper limit of the stochastic region is generally quite far removed from $r = v$, the lower limit is not, and we expect the strongly nonlinear effect of trapping to be important. In RLE Progress Report No. 117 (pp. 193-197) we gave $r > v - \sqrt{a}$ as the condition for trapping; however, it is evident from Fig. X-31b that the stochastic region extends somewhat below the trapping region. Figure X-32 illustrates nicely the distinction between stochastic and trapping regions. The dotted line gives the phase space trajectory of a particle just outside the stochastic region. The solid line above which particles are trapped is

$$r = v - \sqrt{a(1 + \sin(w_2 + v\pi))}. \quad (15)$$

Crosses show the position of a particle starting within the stochastic region but below the trapping region. Note that the ion gains energy slowly and after the fifth cyclotron orbit it is just inside the trapping region. The sixth cyclotron orbit where the particle velocity is roughly doubled has the same characteristics of the trapped orbits discussed in our previous report. In this case, trapping is clearly the most important mechanism by which the ion becomes heated initially. The importance of the initial slow ion heating is that it allows particles closer to the bulk of the ion distribution to become trapped.

Long-Term Effects and Asymptotic State

In order to understand the long-term behavior of the ions, we integrate the equations for 40 particles with velocities just above the lower limit of the stochastic region and with evenly distributed phases. (This is a model for the heating of the tail of the ion distribution.) In Fig. X-33 we plot rms, maximum, and minimum speeds of the

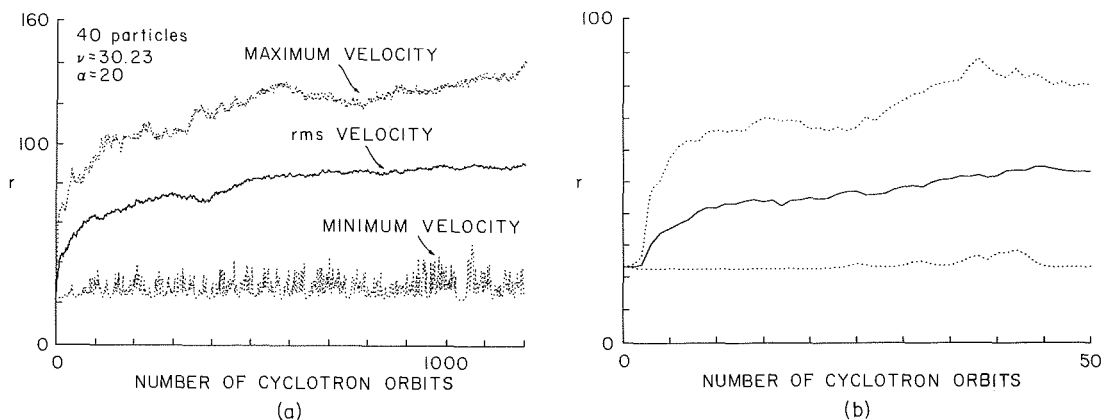


Fig. X-33. (a) Heating of a group of 40 particles with initial velocity $r = 23$ and evenly distributed phases. (b) Same as (a) on an expanded scale.

particles as a function of cyclotron orbit number (which is nearly proportional to time) for $a = 20$ and $\nu = 30.23$. We note that for two or three cyclotron orbits the ions are

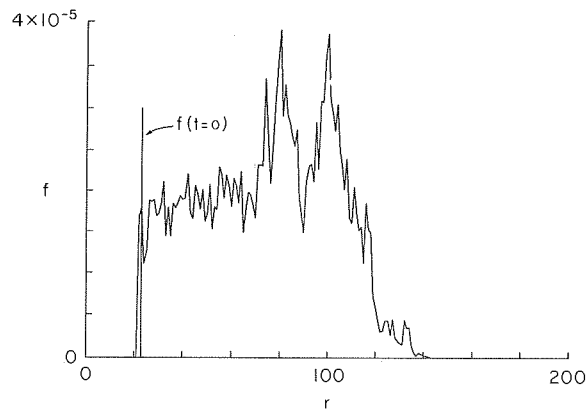


Fig. X-34. Asymptotic distribution function for the particles in Fig. X-33 averaged over cyclotron orbits 900-1200. Normalization is such that $\int_0^{\infty} 2\pi r f dr = 1$. Also shown is the position of the initial δ -function distribution.

heated quite slowly. This is followed by a rapid energy gain as the particles become trapped by the wave, and then by slower heating to an asymptotic rms velocity of approximately 90. The distribution function (Fig. X-34) at this asymptotic state is obtained by averaging over the last 300 cyclotron orbits in Fig. X-33. Note that the effect of the wave is to cause the perpendicular distribution to form a plateau within the stochastic region.

References

1. G. H. Walker and J. Ford, Phys. Rev. 188, 416 (1969).
2. H. Goldstein, Classical Mechanics (Addison-Wesley Press, Inc., Cambridge, Mass., 1951).
3. Equation 12 is identical to the condition for onset of secular perturbations in the particle's phase, and is given by D. J. Sigmar and J. D. Callen, Phys. Fluids 14, 1423 (1971).